Effect of Silver Addition on Cu-based Shape Memory Alloys

L. Liverić,[a] T. Holjevac Grgurić,[b,*] E. Govorčin Bajsić,[c] and M. Kršulja[d]

[a]University of Rijeka, Faculty of Engineering, Vukovarska 58, 51 000 Rijeka, Croatia

[b]Catholic University of Croatia, School of Medicine, Ilica 242, 10 000 Zagreb, Croatia

[c]University of Zagreb, Faculty of Chemical Engineering and Technology, Marulićev trg 19, 10 000 Zagreb, Croatia

[d]Juraj Dobrila University of Pula, Department of Engineering, Zagrebačka 30, 52 100 Pula

doi: https://doi.org/10.15255/CABEQ.2023.2186

Original scientific paper
Received: February 7, 2023
Accepted: September 1, 2023

Shape memory alloys (SMAs) are smart materials with unique properties of superelasticity and shape memory effect. These properties are the consequence of thermoelastic martensitic transformation, which can occur under thermal or mechanical deformation. Cu-Al-Ag alloys have high temperatures of martensite transformation, unlike other SMAs, which makes them suitable for use in specific applications. In this paper, Cu-10Al-1Ag alloy was prepared by melting pure metals in an electric arc furnace and casting the melt in a cylindrical mold. The microstructure of the as-cast and quenched material was determined by optical microscopy (OM) and scanning electron microscopy (SEM) equipped with energy dispersive analysis (EDS). X-ray diffraction (XRD) analysis was performed to identify crystal phases in the microstructure, while transformation temperatures were determined by differential scanning calorimetry (DSC). The hardness of Cu-Al-Ag SMA was also determined with a microhardness tester. The results showed partially formed martensite in the as-cast state, and fully formed martensite structure, 18R-type, in the quenched Cu-10Al-1Ag alloy.

Keywords
shape memory alloys, Cu-Al-Ag alloys, microstructure, phase transformations, martensite

Introduction

Cu-based shape memory alloys (SMAs) show unique properties of superelasticity and shape memory effect, as a consequence of a difusionless reversible martensitic transformation.[1–5] Cu-SMAs are inexpensive and easily processed, so consequently they have a wide range of application, from medical to electronic and electric devices, in the robotics, aerospace industries, etc.[6–11] Both basic Cu-SMAs, Cu-Zn and Cu-Al based, can achieve a thermoelastic martensitic transformation from the high-temperature β-parent phase, austenite phase, by fast cooling or quenching in water. β-Phase decomposes through the eutectoid reaction to $\alpha+\gamma_1$ phase, in equilibrium conditions or by slow cooling.[12–15]

Recently, ternary Cu-Al-Mn SMAs have attracted great interest since the addition of manganese to binary Cu-Al alloy stabilizes and extends the area of β-phase towards the lower aluminum content.[16–18] Therefore, β-phase becomes more stable with respect to diffusional decomposition.[19] During cooling, β-phase undergoes disorder-order transformations $\beta(A2) \rightarrow \beta_2(B2) \rightarrow \beta_1(L2_1)$.[20–25] The body cubic (b.c.c.) superlattice structures can be of the Fe_3Al type (DO_3), CsCl type (B2), and Cu_2MnAl ($L2_1$) type. At low temperatures the spinodal decomposition can occur between DO_3 (Cu_3Al) and $L2_1$ (Cu_2AlMn) phase.[26] The ordering transformation from A2 to $L2_1$ cannot be suppressed at high aluminum concentrations, so $L2_1$ phase, the Heusler alloy (Cu_2AlMn), transforms in a metastable way to 6M martensite. At low aluminum contents, usually below 16 at.%, A2 transforms to A1 (disordered face crystal cubic structure f.c.c.) or 2M structure.[19] Different types of martensite structures can be observed in Cu-based SMAs, depending on the chemical composition: a hexagonal structure 2H and rhombohedral structures 9R, 18R, 6R, 3R.[27–29]

The other most important ternary Cu-based SMAs are Cu-Zn-Al, Cu-Al-Ni, Cu-Al-Be and Cu-Al-Ag.[30–34] The addition of nickel to binary Cu-Al alloys enhances the shape memory effect (SME) and increases the martensite transformation temperature, but the alloy tends to brittle intergranular cracking and shows low cold workability.

*Corresponding author email: tamara.grguric@unicath.hr

Cu-Al-Be SMAs are very cheap for processing, and as low as 0.5–0.56 wt.% of beryllium is enough to achieve SE properties. They show good mechanical properties, high corrosion resistance, and good damping properties.[35] By additional microalloying of SMA, it is possible to obtain better microstructural properties and reduced grain size, especially with the addition of Ti, B, and Si.[36–38] Furthermore, the addition of other elements can improve SME and other functional properties, as well as adjust the temperature of martensitic transformation, which is the key factor for the area of application. Previous investigations of Cu-SMAs were done with microalloying elements such as Cr, Si, Mg, Fe, etc.[39–42]

So far, there has been a limited investigation on the addition of silver to binary Cu-Al SMAs and especially ternary Cu-SMAs. Previous reports have shown that the addition of silver to binary Cu-Al alloys improves the corrosion resistance, increases the martensitic transformation temperature, and enhances the microhardness.[43–46] Cu-Al-Ag SMAs are specific among Cu-based SMAs due to the highest temperature of martensitic transformation, mostly from 200–600 °C, in dependence on the aluminum and silver content, and therefore high-temperature Cu-Al-Ag SMAs have an application in the specific areas.[47,48]

So far, different silver contents in Cu-Al SMAs have been investigated, mostly higher than 5 wt.%. The present study investigated the influence of 1 wt.% silver addition to binary Cu-Al alloys on the microstructure and stability of martensitic transformation.

Materials and methods

Materials

Cu-Al-Ag alloy with 10 wt.% Al and 1 wt.% Ag was prepared by melting in an electric arc furnace, in an argon atmosphere. The pure raw materials were melted: copper (Cu), purity of 99.9 %; aluminum (Al), purity of 99.5 %, and silver (Ag), purity of 99.99 %. The alloy was melted four times for better homogenization, and then cast into a cylindrical mold with a diameter of 8 mm and length of 12 mm. Heat treatment was performed at 900 °C for 30 minutes, followed by quenching in water.

Characterization

Optical and SEM analysis

Samples for microstructure investigations were ground with 600#, 800# and 1200# SiC abrasives, and then polished with 3 µm and 1 µm diamond paste on a grinding-polishing machine TERGAMIN-30 (Struers, Germany). To reveal microstructure, the prepared specimens were etched using a solution of 2.5 g $FeCl_3$/48 mL CH_3OH/10 mL H_2O. The microstructure of SMA was observed using an Axio Vert A1 light microscope (Zeiss, Germany), as well as with a FED QUANTA 250 SEM FEI scanning electron microscope, equipped with an energy dispersive X-ray spectroscopy (EDS) detector (U.K., Oxford).

Hardness

Microhardness of investigated alloys was determined using FM-ARS-9000 fully automatic microhardness measurement system, applying a load of 100 g for a dwell time of 15 seconds. Before the micro-hardness measurements, each sample surface underwent a meticulous preparation process, which included careful cleaning, grinding, and polishing to ensure the accuracy of results. The Vickers micro-hardness values were calculated as the average of five individual measurements taken from each sample.

Differential scanning calorimetry (DSC)

Transformation temperatures were determined by a Mettler-Toledo 822e modulated differential scanning calorimeter. Dynamic measurements were performed in two heating/cooling cycles from –50 °C to 350 °C, in a nitrogen atmosphere, with heating/cooling rate of 10 K min^{-1}.

XRD analysis

XRD analysis was performed with a Bruker D8 Advance diffractometer with CuKα radiation. The scans were collected in the 2θ range of 20–90°, with a 2θ step size of 0.02° and a counting time of 0.6 s, under the accelerating voltage of 40 kV and current of 25 mA.

Results and discussion

Table 1 shows the experimentally determined average overall composition of the prepared sample as determined by EDS. A negligible difference of the designed and experimental composition of Cu-10Al-1Ag SMA can be observed.

Table 1 – *Average composition of SMA alloy determined by SEM-EDS*

	Composition (wt.%)		
Alloy	Cu	Al	Ag
As-cast state	89.46 ±2.46	9.61 ±0.56	0.93 ±0.1

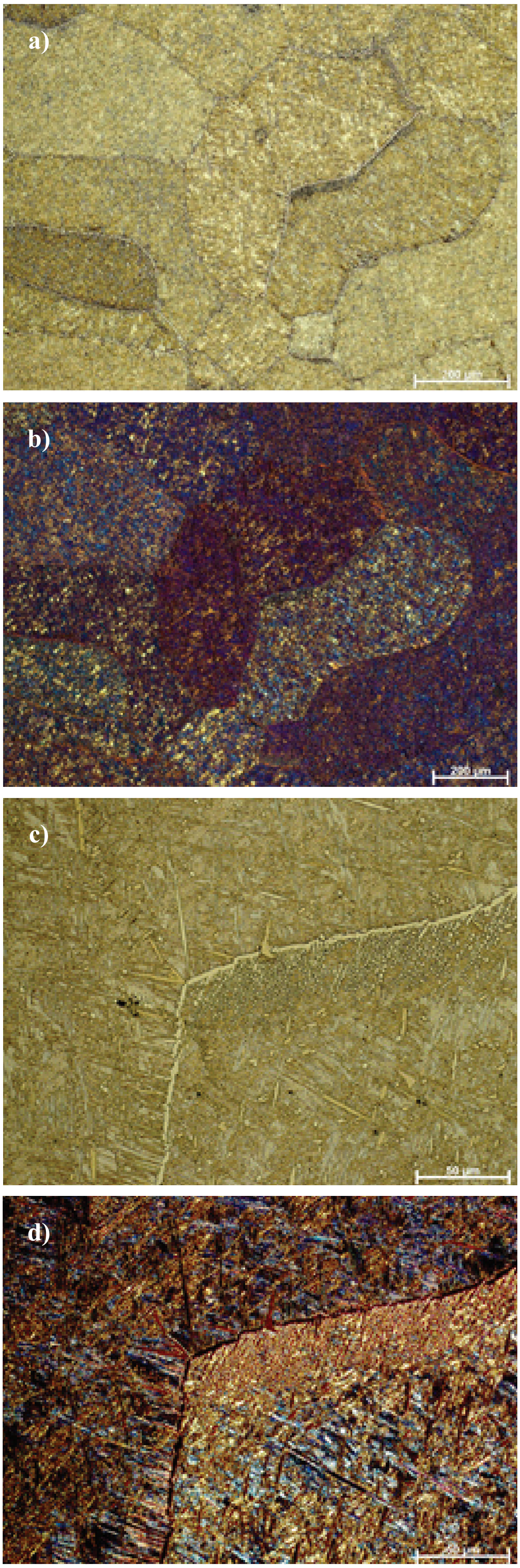

F i g . 1 – *OM micrographs of as-cast Cu-10Al-1Ag shape memory alloy: a) BF, magnification 100x, b) POL, magnification 100x, c) BF, magnification 500x, d) POL, magnification 500x*

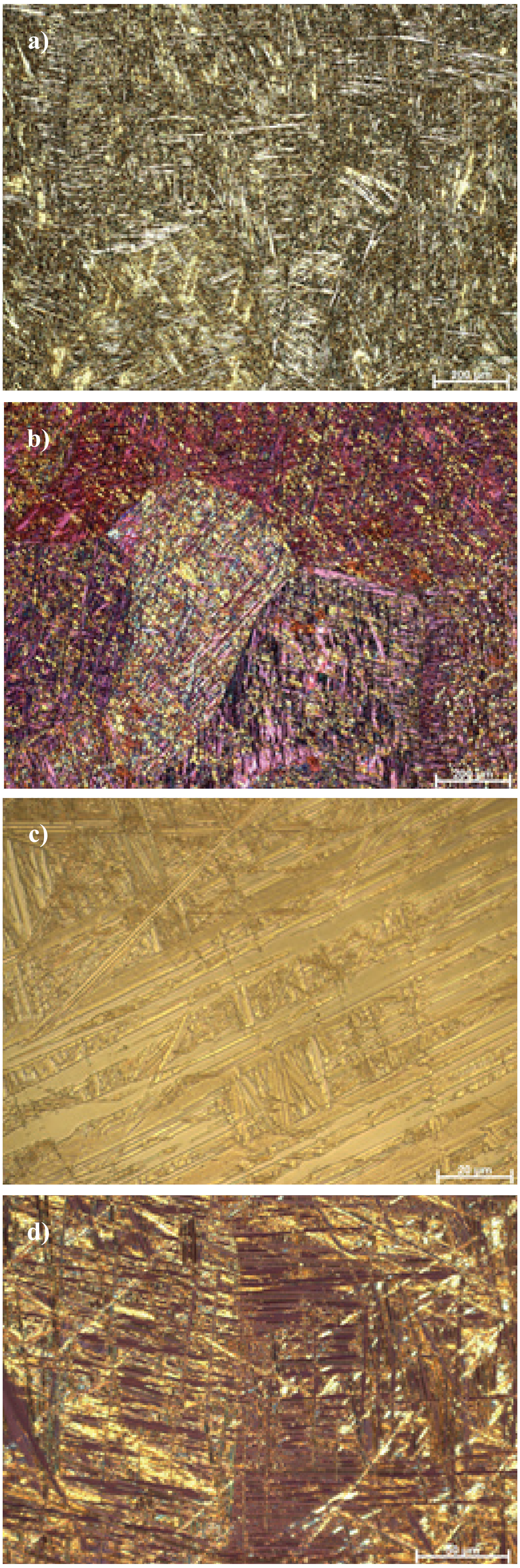

F i g . 2 – *OM micrographs of quenched Cu-10Al-1Ag shape memory alloy: a) BF, magnification 100x, b) POL, magnification 100x, c) BF, magnification 1000x, d) POL, magnification 500x*

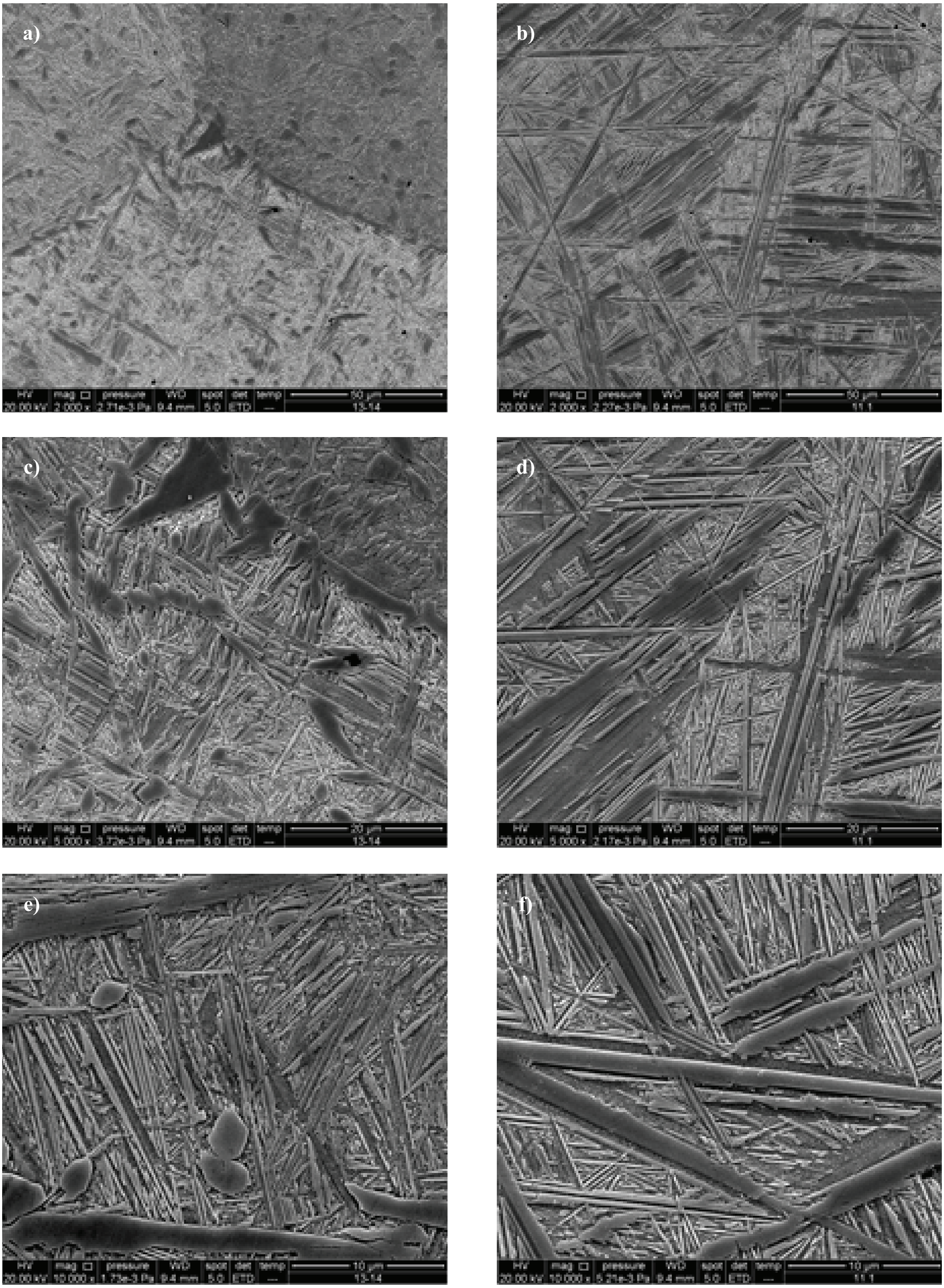

Fig. 3 – *SEM micrograph of Cu-10Al-1Ag shape memory alloy, magnification 2000x: a) as-cast state, b) quenched state, magnification 5000x: c) as-cast state, d) quenched state, and magnification 10000x: e) as-cast state, f) quenched state*

Microstructural analysis of the investigated Cu-Al-Ag alloy in the as-cast state and in the quenched state was carried out by optical microscopy (Figs. 1 and 2), and scanning electron microscopy (Fig. 3). Optical microscopy images are collected in the bright field (BF) and with polarized light (POL). Fig. 1 shows the precipitates of β-parent phase in the microstructure of the as-cast state, and just the beginning of martensite structure formation is observed at the grain boundaries. Inside the grains, short needle-like martensite crystals can be observed, probably of β_1`-type with monoclinic 18R structure, formed from the DO_3 parent phase. In the polarized OM micrographs, the grain boundaries can be seen clearly, with different martensite crystals orientations inside the grains. After quenching, the completely formed martensite structure is observed (Fig. 2). Only β_1`-martensite crystals can be seen, which are formed mostly in the typical zig-zag morphology (Figs. 2 and 3). $\beta_1$`-variants of martensite exhibit thermoelastic behavior due to the controlled growth in self-accommodating zig-zag groups.[49] Figs. 3b), d), and f) show 18R martensite formed as the needle-type and wedge-type crystals.

SEM micrographs of quenched state indicate the existence of only one type of martensite. There are no visible coarse plates of γ_1` martensite, which is the other possible thermally induced martensite in Cu-Al SMAs. The driving force for nucleation of $\gamma_1$` (2H) is higher than for β_1` (18R) martensite. The coexistence of both 18R and 2H structures depends on the alloy composition and the parameters of thermal treatment process. $\beta_1$` and γ_1` have a different morphology due to the different ways of inhomogeneous shear. In the 18R martensite, the inhomogeneous shear occurs by the distributed stacking disorder of the β-parent phase. In 2H martensite, the inhomogeneous shear occurs by twinning on a {1 2 1} plane.[50]

XRD analysis confirmed the existence of only β_1`-martensite phase in the quenched state, and the presence of Cu_3Al and Cu-rich precipitates in the as-cast state (Fig. 6).

EDS analysis (Fig. 4) showed that, in the as-cast Cu-10Al-1Ag alloy, beside β-parent phase and martensite, there were no visible precipitates of pure silver, which were reported previously for samples having higher silver contents.[51] EDS analysis of quenched state is given in Fig. 5.

The quenched Cu-10Al-1Ag alloy shows lower microhardness in relation to the as-cast state (Table

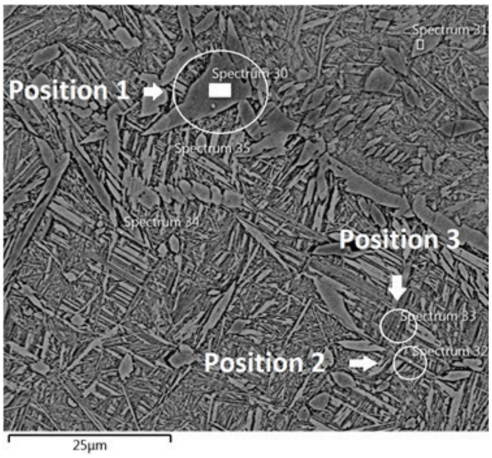

Position 1

Element	Wt%
Al	8.82 ±0.25
Cu	88.17 ±0.70
Ag	1.40 ±0.23

Position 2

Element	Wt%
Al	9.87 ±0.46
Cu	83.39 ±1.30
Ag	1.27 ±0.40

Position 3

Element	Wt%
Al	11.29 ±0.50
Cu	88.04 ±0.55
Ag	0.00

Fig. 4 – *EDS analysis of as-cast Cu-10Al-1Ag alloy*

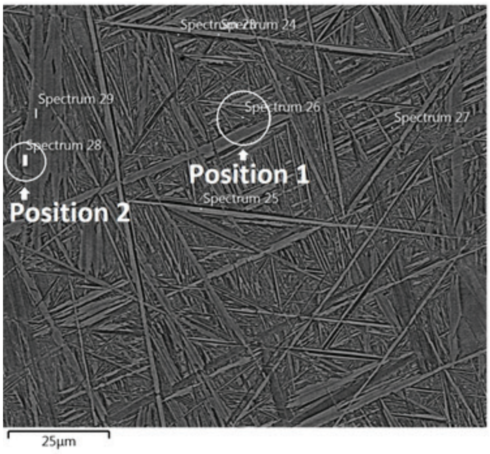

Position 1

Element	Wt%
Al	10.92 ±0.46
Cu	88.00 ±0.59
Ag	1.09 ±0.42

Position 2

Element	Wt%
Al	10.90 ±0.51
Cu	88.17 ±0.64
Ag	0.93 ±0.44

Fig. 5 – *EDS analysis of quenched Cu-10Al-1Ag alloy at different positions*

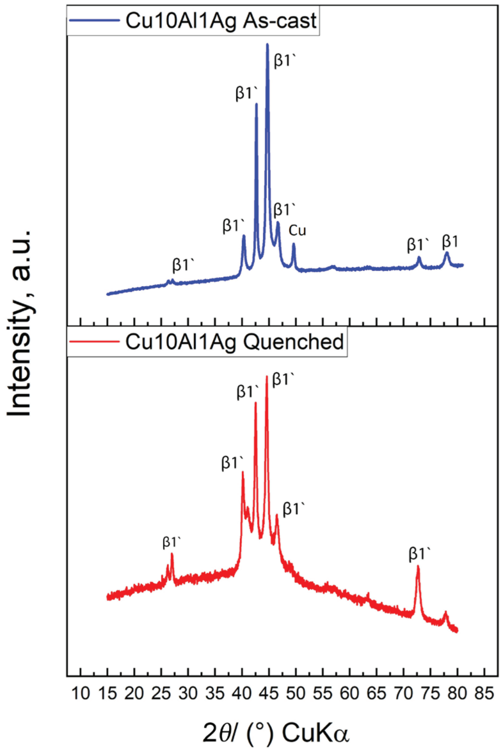

Fig. 6 – *XRD diffractogram of Cu-10Al-1Ag SMA alloy*

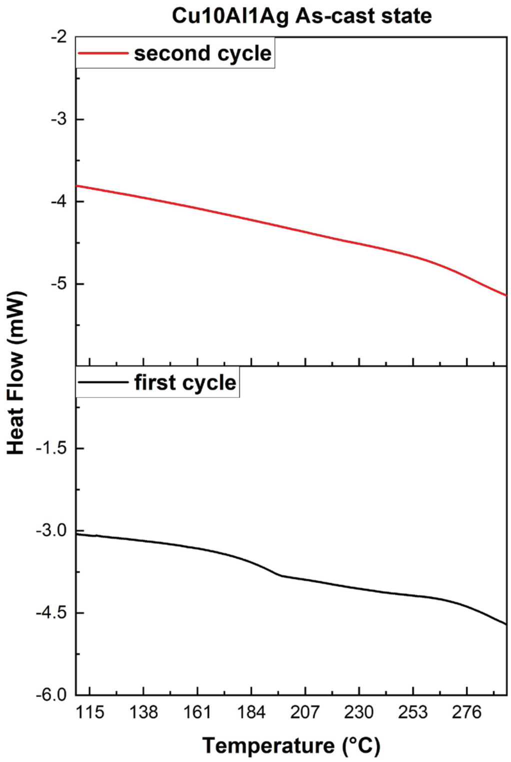

Fig. 7 – *DSC thermograms of as-cast Cu-10Al-1Ag shape memory alloy*

Table 2 – *Microhardness of Cu–Al–Ag SMA alloy*

Hardness	HV					
Cu10Al1Ag	1	2	3	4	5	Average
As-cast state	314.94	292.65	284.43	295.89	307.84	297.34
Quenched state	278.57	284.55	270.88	269.11	280.45	278.00

2), in agreement with the previous investigations of SMAs.[52] The small difference in hardness between the as-cast and quenched states may be attributed to mechanically induced martensite formation in the stressed regions that occurs under high indenter loading.[53] Despite the microstructural changes that the alloy undergoes during quenching, there is no significant change in hardness. Probably due to the low Ag content in the SMA composition.

The results of DSC analysis are shown in Figs. 7–10. The DSC thermogram for as-cast Cu-Al-Ag alloy shows, after the first cycle, an endothermic transformation with the start temperature of austenite transformation A_s = 176 °C and finish temperature of austenite transformation A_f = 225 °C. After the second heating, transformation is barely detectable (Fig. 7). The martensite transformation is observed in cooling curves with start and finish temperatures of martensite transformation, M_s = 182 °C and M_f = 154 °C (in the first cooling cycle), and 151 °C (in the second cooling cycle) (Fig. 9).

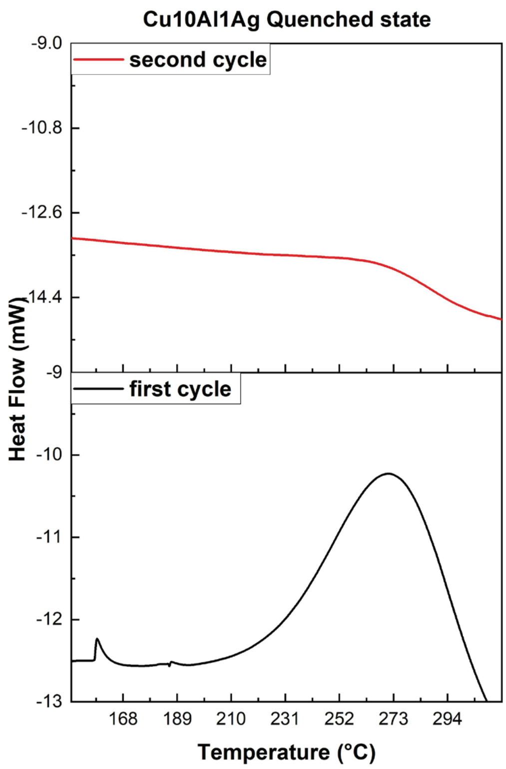

Fig. 8 – *DSC thermograms of quenched Cu-10Al-1Ag shape memory alloy*

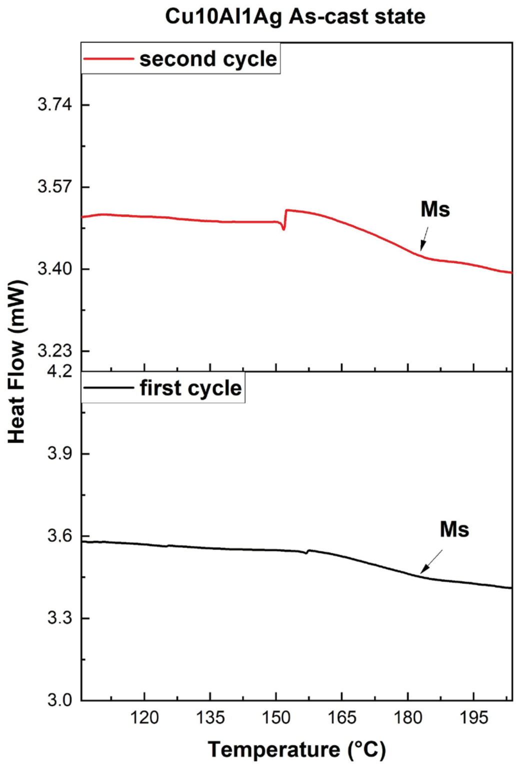

Fig. 9 – *Martensite transformation for as-cast Cu-10Al-1Ag shape memory alloy*

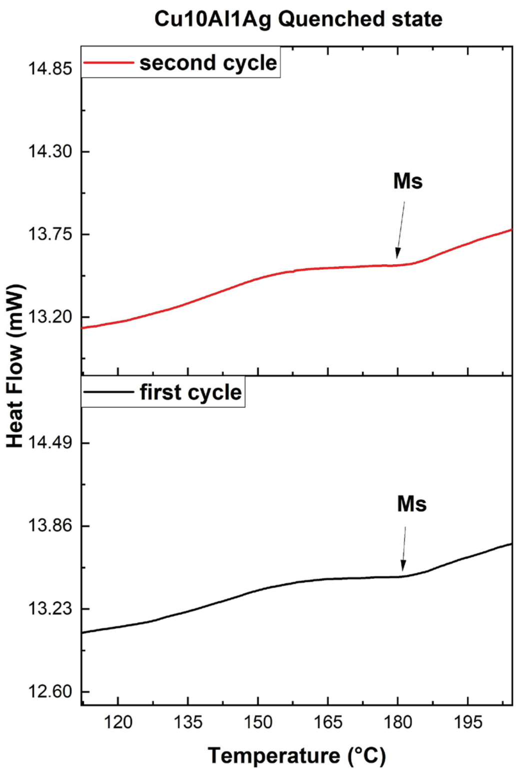

Fig. 10 – *Martensite transformation for quenched Cu-10Al-1Ag shape memory alloy*

After quenching, austenite transformation is not detectable at DSC heating curves, while martensitic transformation shows start martensitic temperature at M_s = 180 °C and finish transformation temperature M_f = 132 °C. Martensitic transformation temperatures did not change significantly in the first and second cycle (Figs. 8, 10). In relation to as-cast alloy, start martensite temperature is similar, but transformation releases higher heat fusion, and finish transformation temperature is shifted to lower value. DSC results indicate that the formed β_1`-martensite is thermally stable, which is very important for the application of SMA. The microstructural and phase analysis, as well as DSC results showed that the shape memory properties of material can be achieved with only 1 wt.% of added silver, with the stable martensite phase and very high transformation temperatures.

Conclusion

Cu-10Al-1Ag alloy was successfully prepared by smelting pure metals in an electric arc furnace. The results showed partial formation of martensitic structure in the as-cast state, and completely formed martensite phase after quenching in water. Only one type of the martensite structure was found with microstructural investigations, i.e. monoclinic 18R or β_1` structure. The martensite transformation temperature was found in the range of 180 °C to 130 °C. Therefore, a very small amount of added silver of only 1 wt.% leads to achieving shape memory properties in Cu-Al-Ag alloy.

List of abbreviations and symbols:

SMA – shape memory alloy
OM – optical microscope
SEM – scanning electron microscope
EDS – energy dispersive X-ray spectroscopy
DSC – differential scanning calorimetry
XRD – X-ray diffraction
M_s – temperature at which the transformation of martensite begins (starts), °C
M_f – temperature at which the transformation of martensite is completed (finished), °C
A_s – temperature at which the transformation of austenite begins (starts), °C
A_f – temperature at which the transformation of austenite is completed (finished), °C
BF – bright field
POL – polarized light

References

1. *Mazzer, E. M., da Silva, M. R., Gargarella, P.,* Revisiting Cu-based shape memory alloys: Recent developments and new perspectives, J. Mater. Res. **37(1)** (2022) 162.
doi: https://doi.org/10.1557/s43578-021-00444-7
2. *Salgado, R. S., Silva, L. S., Oliveira, L. M., Mamani, T. P. Q., Silva, R. A. G.*, Non-isothermal kinetics and the effects of alloying elements on bainite precipitation in the Cu74.5Al15.0Mn10.5 alloy, Thermochim. Acta **711** (2022) 179214
doi: https://doi.org/10.1016/j.tca.2022.179214
3. *Silva, L. S., Silva, R. A. G.*, Alloys-by-design: Role of atomic properties on the phase equilibria of CuAlMn-based alloys, Mater. Charact. **163** (2020) 110304.
doi: https://doi.org/10.1016/j.matchar.2020.110304
4. *Silva, R. A. G., Adorno, A. T., Carvalho, T. M., Magdalena, A. G., Santos, C. M. A.*, Precipitation reaction in alpha-Cu-Al-Ag Alloys, Rev. Mat. **16(3)** (2012) 747.
doi: https://doi.org/10.1590/S1517-70762011000300002
5. *Grgurić, T. H., Manasijević, D., Kožuh, S., Ivanić, I., Anžel, I., Kosec, B., Bizjak, M., Bajsić, E. G., Balanović, Lj., Gojić, M.*, The effect of the processing parameters on the martensitic transformation of Cu-Al-Mn shape memory alloy, J. Alloys Compd. **765** (2018) 664.
doi: https://doi.org/10.1016/j.jallcom.2018.06.250
6. *Dasgupta, R., Pandey, A.*, *Hussain, S., Jain, A. K., Ansari, A., Sampath, V.,* Effect of microstructure on roll-ability and shape memory effect in Cu- based shape memory alloys, Applied Innovation Research **1** (2019) 29.
doi: https://nopr.niscair.res.in/handle/123456789/45840
7. *Dasgupta, R.*, A Look into Cu-based shape memory alloys: Present scenario and future prospects, J. Mater. Res. **29(16)** (2014) 1681.
doi: https://doi.org/10.1557/jmr.2014.189
8. *Deniz Çirak, Z., Kök, M., Aydoğdu, Y.,* The Effect of chromium addition on physical properties of Cu-Al based high temperature shape memory alloy, Arch. Metall. Mater. **63(4)** (2018) 1595.
doi: https://doi.org/10.24425/amm.2018.125082
9. *Firstov, G. S., Kosorukova, T. A., Koval, Y. N., Odnosum, V. V.*, High entropy shape memory alloys, materials today, Proceedings **2(S3)** (2015) S499.
doi: https://doi.org/10.1016/j.matpr.2015.07.335
10. *Manasijevic, D., Holjevac Grguric, T., Balanovic, Lj., Stamenkovic, U., Gorgievski, M., Gojic, M.,* Effect of Mn content on the microstructure and phase transformation temperatures of the Cu-Al-Mn-Ag shape memory alloys, Kovove Mater. **58** (2020) 293.
doi: https://doi.org/10.4149/km_2020_4_293
11. *Živković, D., Holjevac Grgurić, T., Gojić, M., Ćubela, D., Stanojević Šimišić, Z., Kostov, A., Kožuh, S.*, Calculation of thermodynamic properties of Cu–Al–(Ag, Au) shape memory alloy systems, Trans. Indian Instit. Met. **67(2)** (2014) 285.
doi: https://doi.org/10.1007/s12666-013-0328-9
12. *Stanojević Šimšić, Z., Živković, D., Manasijević, D., Holjevac Grgurić, T., Du, Y., Gojić, M., Todorović, R.,* Thermal analysis and microstructural investigation of Cu-rich alloys in the Cu–Al–Ag system, J. Alloys Compd. **612** (2014) 486.
doi: https://doi.org/10.1016/j.jallcom.2014.05.070
13. *Stanojević Šimšić, Z., Manasijević, D., Živković, D., Holjevac Grgurić, T., Kostov A., Minić, D., Živković, Ž.*, Experimental investigation and characterization of selected as-cast alloys in vertical Cu0.5Ag0.5–Al section in ternary Cu–Al–Ag system, J. Therm. Anal. Calorim. **120(1)** (2015) 149.
doi: https://doi.org/10.1007/s10973-015-4576-2
14. *Huang, H. Y., Zhu, Y. Z., Chang, W. S.,* Comparison of bending fatigue of NiTi and CuAlMn shape memory alloy bars, Adv. Mater. Sci. Eng. (2020) 8024803.
doi: https://doi.org/10.1155/2020/8024803
15. *Stošić, Z., Manasijević, D., Balanović, Lj., Holjevac Grgurić, T.*, Effects of composition and thermal treatment of Cu-Al-Zn alloys with low content of Al on their shape-memory properties, Mater. Res. **20(5)** (2017) 1425.
doi: https://doi.org/10.1590/1980-5373-MR-2017-0153
16. *Silva, R. A. G., Paganotti, A., Adorno, A. T., Santos, C. M. A., Carvalho, T. M.,* Characteristics of the Cu–18.84 at.% Al–10.28 at.% Mn–1.57 at.% Ag alloy after slow cooling from high temperatures, J. Thermal. Anal. Calorim. **121** (2015) 1233.
doi: https://doi.org/10.1007/s10973-015-4654-5
17. *Mallik, U. S., Sampath, V.*, ˙Effect of alloying on microstructure and shape memory characteristics of Cu-Al-Mn shape memory alloys, Mater. Sci. Eng. A **481–482** (2008) 680.
doi: https://doi.org/10.1016/j.msea.2006.10.212
18. *Praveen, N., Mallik, U. S., Shivasiddaramaiah, A. G., Reddy, G. N. N.,* A study on material removal rate of Cu-Al-Mn shape memory alloys in WEDM, Mater. Today – Proceedings **46** (2012) 2770.
doi: https://doi.org/10.1016/j.matpr.2021.02.555
19. *Santos, C. M. A., Adorno, A. T., Oda, N. Y., Sales, B. O., Silva, L. S., Silva, R. A. G.,* Phase transformations and aging of the Cu72.9Al15.0Mn10.5Ag1.6 alloy, J. Alloy. Compd. **685** (2016) 587.
doi: https://doi.org/10.1016/j.jallcom.2016.05.303
20. *Motta, M. B. J. L., Adorno, A. T., Santos, C. M. A., Silva, R. A. G.,* Kinetics of bainite precipitation in the Cu69.3Al18.8Mn10.3Ag1.6 alloy, Mater. Chem. Phys. **188** (2017) 125.
doi: https://doi.org/10.1016/j.matchemphys.2016.12.019
21. *Silva, R. A. G., Paganotti, A., Gama, S., Adorno, A. T., Carvalho, T. M., Santos, C. M. A.,* Investigation of thermal, mechanical and magnetic behaviors of the Cu-11% Al alloy with Ag and Mn additions, Mater. Charact. **75** (2013) 194.
doi: https://doi.org/10.1016/j.matchar.2012.11.007
22. *Xi, X., Zhang, J., Tang, H., Cao, Y., Xiao, Z.,* The ultrahigh functional response of CuAlMnNb shape memory alloy by selective laser melting, J. Mater. Res. Tech. **20** (2022) 671.
doi: https://doi.org/10.1016/j.jmrt.2022.07.091
23. *Santos, C. M. A., Adorno, A. T., Paganotti, A., Silva, C. C. S., Oliveira, A. B., Silva, R. A. G.*, Phase stability in the Cu-9 wt%Al-10 wt%Mn-3 wt%Ag alloy, J. Phys. Chem. Solids **104** (2017) 145.
doi: https://doi.org/10.1016/j.jpcs.2017.01.012
24. *Pilz, C. B., Matsumura, E. L., Paganotti, A., Cornejo, D. R., Silva, R. A. G.*, Microstructure and phase stability of CuAlMnAgZr multicomponent alloys, Mater. Chem. Phys. **241** (2020) 122343.
doi: https://doi.org/10.1016/j.matchemphys.2019.122343
25. *Zhu, J. J., Liew, K. M.*, Description of deformation in shape memory alloys from DO3 austenite to 18R martensite by group theory, Acta Mater. **51(9)** (2003) 2443.
doi: https://doi.org/10.1016/S1359-6454(02)00604-3
26. *Velázquez, D., Chaparro, M. A. E., Böhnel, H. N., Romero, R., Lanzini, F.,* Spinodal decomposition, chemical and magnetic ordering in Cu–Al–Mn shape memory alloys, Mater. Chem. Phys. **246** (2020) 122793.
doi: https://doi.org/10.1016/j.matchemphys.2020.122793
27. *Suru, M. G., Lohan, N. M., Pricop, B., Mihalache, M., Mocanu, M., Bujoreanu L. G.,* Precipitation effects on the martensitic transformation in a Cu-Al-Ni shape memory alloy, J. Mater. Eng. Perform. **25(4)** (2016) 1562.
doi: https://doi.org/10.1007/s11665-016-1981-z

28. *Zárubová, N., Novák, V.,* Phase stability of CuAlMn shape memory alloys, Mater. Sci. Eng. A **378** (2004) 216. doi: https://doi.org/10.1016/j.msea.2003.10.346
29. *Qian, S., Geng, Y., Wang, Y., Pillsbury, T. E., Hada, Y., Yamaguchi, Y., Fujimoto, K., Hwang, Y., Radermacher, R., Cui, J., Yuki, Y., Toyotake, K., Takeuchi, I.,* Elastocaloric effect in CuAlZn and CuAlMn shape memory alloys under compression, Philos. Trans. Royal Soc. A **374(2074)** (2016) 20150309. doi: https://doi.org/10.1098/rsta.2015.0309
30. *Saud, S. N., Hamzah, E., Abubakar, T., Bakhsheshi-Rad, H. R., Farahany, S., Abdolahi, A., Taheri, M. M.,* Influence of Silver nanoparticles addition on the phase transformation, mechanical properties and corrosion behaviour of Cu–Al–Ni shape memory alloys, J. Alloys Compd. **612** (2014) 471. doi: https://doi.org/10.1016/j.jallcom.2014.05.173
31. *Guilemany, J. M., Fernandez, J., Zhang, X. M.,* TEM study on the microstructure of Cu–Al–Ag shape memory alloys, Mater. Sci. Eng. A **438** (2006) 726. doi: https://doi.org/10.1016/j.msea.2006.02.089
32. *Karaduman, O., Ozkul, I.,* Kinetic and structural study on CuAlMnNi shape memory alloy with a novel composition, Adv. Eng. Sci. **1(1)** (2021) 13. doi: https://publish.mersin.edu.tr/index.php/ades/article/view/21
33. *Santos, C. M. A., Adorno, A. T., Stipcich, M., Cuniberti, A., Souza, J. S., Bessa, C. V. X., Silva, R. A. G.,* Effects of Ag presence on phases separation and order-disorder transitions in Cu-xAl-Mn alloys, Mater. Chem. Phys. **227** (2019) 184. doi: https://doi.org/10.1016/j.matchemphys.2019.02.016
34. *Saud, S. N., Hamzah, E., Abubakar, T., Bakhsheshi-Rad, H. R.,* Microstructure and corrosion behaviour of Cu–Al–Ni shape memory alloys with Ag nanoparticles, Mater. Corr. **66(6)** (2015) 527. doi: https://doi.org/10.1002/maco.201407658
35. *Figueroa, C. G., Jacobo, V. H., Cortés-Pérez, J., Schouwenaars, R*., Surface nanostructuring of a CuAlBe shape memory alloy produces a 10.3 ± 0.6 GPa nanohardness martensite microstructure, Materials **13(24)** (2020) 1. doi: https://doi.org/10.3390/ma13245702
36. *Souza, J. S., Oliveira, M. C. L., Antunes, R. A., Silva, R. A. G.*, Effects of Sn, Gd, and Mn additions on the surface chemistry and electrochemical behavior of CuAl-based alloys in sodium chloride solution, Appl. Surf. Sci. **573** (2022) 151488. doi: https://doi.org/10.1016/j.apsusc.2021.151488
37. *Canbay, C. A.,* Investigation of thermoelastical martensitic transformations and structure in new composition of CuAlMnTi shape memory alloy, J. Mater. Electron. Device **1** (2019) 60. www.dergi-fytronix.com/index.php/jmed/article/view/45
38. *Canbay, C. A., Karagoz, Z.,* The effect of quaternary element on the thermodynamic parameters and structure of CuAlMn shape memory alloys, Appl. Phys. A **113(1)** (2013) 19. doi: https://doi.org/10.1007/s00339-013-7880-3
39. *Chang, S. H., Liao, B. S., Gholami-Kermanshahi, M.,* Effect of Co additions on the damping properties of Cu-Al-Ni shape memory alloys, J. Alloys Compd. **847** (2020) 156560. doi: https://doi.org/10.1016/j.jallcom.2020.156560
40. *Wang, Q., Yao, C., Lu, D., Yin, F.,* Effect of combined use of inoculation and hot rolling on microstructures and damping property of a Cu-Al-Ni-Mn-Ti shape memory alloy, Mater. Lett. **330** (2023) 133392. doi: https://doi.org/10.1016/j.matlet.2022.133392
41. *Ferreira, R. O., Silva, L., Silva, R. A. G.*, Thermal behavior of as-annealed CuAlMnAgZr alloys, J. Therm. Anal. Calorim. **146** (2021) 595. doi: https://doi.org/10.1007/s10973-020-10002-8
42. *Shyi-Kaan, W., Wei-Jyun, C., Shih-Hang, C.,* Damping characteristics of inherent and intrinsic internal friction of Cu-Zn-Al shape memory alloys, Metals **7(397)** (2017) 1. doi: https://doi.org/10.3390/met7100397
43. *Corral-Bustamante, R. L., Trevizo, M. A. F., Hernandez-Magdaleno, J. N.,* Modeling of shape memory alloys for medical design in robotics, Manuf. Sci. Technol. **3(4)** (2015) 82. doi: https://doi.org/10.13189/mst.2015.030402
44. *Silva, R. A. G., Paganotti, A., Adorno, A. T., Santos, C. M. A, Carvalho T. M.*, Precipitation hardening in the Cu – 11 wt.% Al – 10 wt.% Mn alloy with Ag addition, J. Alloys Compd. **10** (2015) 13. doi: https://doi.org/10.1016/j.jallcom.2014.12.208
45. *Pinto, R. D. A., Ferreira, L. D. R., Silva, R. A. G.,* Size matters: Influence of atomic radius from the ternary addition on the properties of Cu79Al19X2 (X = Be, Mn, Ag) alloys, Mater. Chem. Phys. **294** (2021) 127021. doi: https://doi.org/10.1016/j.matchemphys.2022.127021
46. *Krishna, T. S. V., Rao, D. S.,* Effect of aluminium on microstructure and shape memory effect in Cu-Al-Ag-Mn shape memory alloys, Aust. J. Mech. Eng. (2022). doi: https://doi.org/10.1080/14484846.2022.2105467
47. *Fernándeza, J., Isalgue, I., Franch, R.,* Effect of thermal cycling on CuAlAg shape memory alloys, Mater. Today-Proceeding **2S** (2015) S805. doi: https://doi.org/10.1016/j.matpr.2015.07.404
48. *Ferreira, R. O., Silva, L. S., Silva, R. A. G.,* Thermal behavior of as-annealed CuAlMnAgZr alloys, J. Therm. Anal. Calorim. **146(2)** (2021) 595. doi: https://doi.org/10.1007/s10973-020-10002-8
49. *Sarı, U., Aksoy, I.,* Electron microscopy study of 2H and 18R martensites in Cu–11.92 wt.% Al–3.78 wt.% Ni shape memory alloy, J. Alloys Compd. **417** (2006) 138. doi: https://doi.org/10.1016/j.jallcom.2005.09.049
50. *Aldırmaz, E., Aksoy, I.,* Effects of heat treatment and deformation on 2H and 18R martensites in Cu–9.97 % Al–4.62 % Mn alloy, Arab. J. Sci. Eng. **39** (2014) 575. doi: https://doi.org/10.1007/s13369-013-0871-z
51. *Arruda, G. J., Adorno, A. D., Benedetti, A. V., Fernandez, J., Guilemany, J. M*., Influence of silver additions on the structure and phase transformation of the Cu-13 wt.% Al alloy, J. Mater. Sci. **32** (1997) 6299. doi: https://doi.org/10.1023/A:1018601614224
52. *Kožuh, S., Gojić, M., Ivanić, I., Holjevac Grgurić, T., Kosec, B., Anžel, I.,* The effect of heat treatment on the microstructure and mechanical properties of Cu-Al-Mn shape memory alloy, Kem. Ind. **67(1-2)** (2018) 11. https://urn.nsk.hr/urn:nbn:hr:115:351667
53. *Ćorić, D., Franz, M.,* Properties of thermally treated CuZn27Al3 shape memory alloy, J. Mech. **55(10)** (2009) 623. https://www.sv-jme.eu/article/properties-of-thermally-treated-cuzn27al3-shape-memory-alloy